Thermomechanical intermodulation noise in cavity optomechanics

S. A. Fedorov,[1,*] A. Beccari,[1,*] A. Arabmoheghi,[1]
M. J. Bereyhi,[1] D. J. Wilson,[2] N. J. Engelsen,[1] and T. J. Kippenberg[1,†]

[1] *Institute of Physics (IPHYS), École Polytechnique Fédérale de Lausanne, 1015 Lausanne, Switzerland*
[2] *College of Optical Sciences, University of Arizona, Tucson, Arizona 85721, USA*

(Dated: December 17, 2019)

Cavity optomechanics in the weak coupling regime when single-photon coupling rate is much smaller than the optical linewidth is conventionally described by linearly interacting optical and mechanical modes. Yet dispersive optomechanical interaction is inherently nonlinear, and the effects of this nonlinearity can be far from negligible even for weakly coupled systems. The nonlinearity of optomechanical interaction results in mixing of different frequency components of the thermomechanical noise and the emergence of broadband thermal noise at frequencies and in the field quadratures where it does not get transduced linearly. In order to illustrate this effect, we study the noise properties of an optomechanical membrane in the middle cavity at room temperature. Using an optical cavity with finesse $\mathcal{F} = 1.5 \times 10^4$ and a low effective mass soft clamped mode with $Q = 4. \times 10^7$ as a mechanical oscillator we are able to operate at nominal quantum cooperativity equal to one. In this regime, the amplitude fluctuations of intracavity light due to the thermal intermodulation noise exceed the vacuum fluctuations by tens of dB, which makes it challenging to observe quantum aspects of optomechanical interaction.

I. INTRODUCTION

Interferometric position measurements achieve exceptional resolution by transducing mechanical displacements into optical phase shifts. The resolution can be high enough so that the disturbance of mechanical motion due to the fundamental quantum back-action of measurement becomes significant, and the optomechanical interaction enters quantum regime. High-finesse optical cavities is a key tool that increases the sensitivity of interferometric measurements and enhances the strength of optomechanical coupling by allowing the probe light to interact with the mechanical system multiple times. However, an increase in the measurement sensitivity provided by a cavity comes at the price of a reduced dynamic range, Δx_d, given by[1, 2]

$$\Delta x_d = \lambda/\mathcal{F}, \tag{1}$$

where λ is optical wavelength and $\mathcal{F}$ is the cavity finesse. Finite dynamic range results in nonlinear conversion of mechanical displacements to the measured signal and can significantly obscure the the measurement record even when the total fluctuations are much smaller than the cavity linewidth.

To the lowest order in the displacement over dynamic range, nonlinearity manifests as the measurement of mechanical displacement squared. Such measurements potentially have enticing applications in cavity optomechanics, they could be used for the observation of phononic jumps[3], phononic shot noise[4], and the creation of mechanical squeezed states[5] if the effects of linear measurement backaction is possible to make small[6, 7]. Experiments demonstrating quadratic optomechanical position measurements using genuine position-squared coupling[8] up to date remain deeply in the classical regime. The nonlinearity of displacement measurements can produce quadratic measurement rates that are orders of magnitude higher[7], but this mechanism is inevitably accompanied by linear quantum backaction. Nonlinear transduction of thermomechanical noise was observed in optomechanical systems previously[7, 9] and it was suggested that the nonlinearity of cavity transduction can be used as a resource for engineering non-Gaussian states of the mechanical oscillator[7].

Despite potentially being useful as a resource, the nonlinear transduction of mechanical motion introduces new challenges in experiments exploiting the linear optomechanical interation, including the observation of ponderomotive squeezing[10, 11] or ground state cooling of a mechanical oscillator[12–14]. Such experiments typically require the broadband fluctuations of intracavity light to be limited by the vacuum fluctuations, whereas the nonlinearly transduced thermomechanical motion appears as extraneous noise. In optomechanical systems it is typical that multiple mechanical modes are coupled to the same optical mode, even if only one mechanical mode is of interest in the end, the experiments in our work are also in this regime. For multimode systems the nonlinear conversion of total thermal motion is dominated by intermodulation products between different modes (as illustrated in Fig. 1a-b), therefore we refer to the extraneous noise created by this process as intermodulation noise.

The thermal intermodulation noise is particularly problematic for multimode optomechanical systems at high temperature, for which the total magnitude of thermal noise is large. From the perspective of linear optomechanics, the effect of elevated temperature can always be compensated by increasing the optical power so that optomechanical coupling rate compensates for the increased mechanical decoherence. Moreover, it is often sufficient

* These authors contributed equally
† tobias.kippenberg@epfl.ch

that the fluctuations of optical field are quantum limited in a small frequency band around the mechanical resonance of interest. In presence of transduction nonlinearity, at the same value of quantum cooperativity the added intermodulation noise is larger for high absolute magnitudes of thermal noises. The intermodulation noise could be one reason why the observation of quantum aspects of optomechanical interaction at room temperature is very challenging and has only been achieved in a handful of experiments[15–19], most of which[17–19] operated in an exotic regime when the radiation pressure spring exceeds the natural frequency of the oscillator by two orders of magnitude.

One platform that is considered promising for attaining the quantum regime optomechanic interaction at room temperature is membrane in the middle system[20, 21]. Utilizing recently developed high-Q and low mass soft-clamped[25, 26] mechanical resonators, quantum-backaction dominated regime is predicted to be reacheable at microwatt input optical powers. Still, due to the high density of mechanical modes in membrane resonators this system is strongly limited by the intermodulation noise.

The manuscript is structured as follows. In the beginning we introduce a theoretical model of classical thermomechanical noise intermodulation in an optomechanical cavity. Then we present measurements in low-cooperativity regime which show that the intermodulation noise is a major source of extraneous noise in a membrane-in-the-middle experiment at room temperature. Finally, employing a PnC membrane with a low effective mass soft clamped mode we conduct measurements the regime $C_q \sim 1$ and show that the intermodulation noise poses a significant limitation for the observability of quantum backaction-imprecision correlations in such system.

II. NONLINEAR TRANSDUCTION OF OPTOMECHANICAL SIGNALS IN CLASSICAL REGIME

The cavity-induced nonlinearity of optomechanical interaction was studied in the works[7, 9, 23]. Nevertheless, possibly because this effect is not readily apparent from the optomechanic Hamiltonian, made it receive little attention in the literature. This is despite the observation that nonlinear transduction can produce signals, quadratic in mechanic displacement, that are orders of magnitude stronger than those from the conventionally considered $\partial^2\omega_c/\partial x^2$ term[7]. Below we derive the classical dynamics of optical field in an optomechanical cavity taking into account terms that are quadratic in displacement. We show that in membrane in the middle cavity typical quadratic signals originating from the nonlinear transduction are $r\mathcal{F}$ larger than the signals due to the nonlinear optomechanical coupling, $\partial^2\omega_c/\partial x^2$.

We first show how transduction nonlinearity emerges

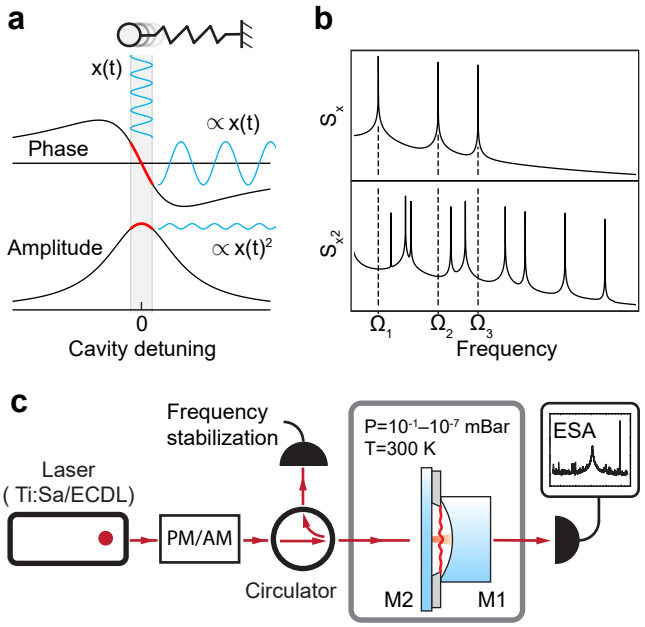

FIG. 1. a) Transduction of the oscillator motion to the phase (upper panel) and amplitude (lower panel) of resonant intracavity light. b) Spectra of linear (upper panel) and quadratic (lower panel) position fluctuations of a multimode system. c) Experimental setup.

in a generic optomechanic system and evaluate the signal strength. We consider a two-port optomechanic cavity driven by laser from port 1, and assume fast cavity limit, which corresponds to the cavity decay constant κ being much larger than the frequency of mechanical fluctuations. The classical dynamics of optical field inside the cavity is described by the equation

$$\frac{da(t)}{dt} = \left(i\Delta(t) - \frac{\kappa}{2}\right) a(t) + \sqrt{\kappa_1}\, s_{1,\mathrm{in}}, \tag{2}$$

where $\Delta = \omega_L - \omega_c$ is the laser detuning from the cavity resonance, modulated by the mechanical motion. In adiabatic limit, if the cavity field adiabatically follows the fluctuations of $\Delta(t)$, the intracavity field is found as

$$a(t) = \frac{2}{\sqrt{\kappa}}\sqrt{\eta_1} L(\delta(t))\, s_{1,\mathrm{in}}, \tag{3}$$

where we introduced the normalized detuning $\delta = 2\Delta/\kappa$, the cavity decay ratio $\eta_{1,2} = \kappa_{1,2}/\kappa$ and Lorentzian susceptibility

$$L(\delta) = \frac{1}{1 - i\delta}. \tag{4}$$

Assuming the laser to be resonant with the cavity on average and expanding L in small δ up to the second order we get

$$a(t) = \frac{2}{\sqrt{\kappa}}\sqrt{\eta_1}(1 - i\delta(t) - \delta(t)^2) s_{1,\mathrm{in}}. \tag{5}$$

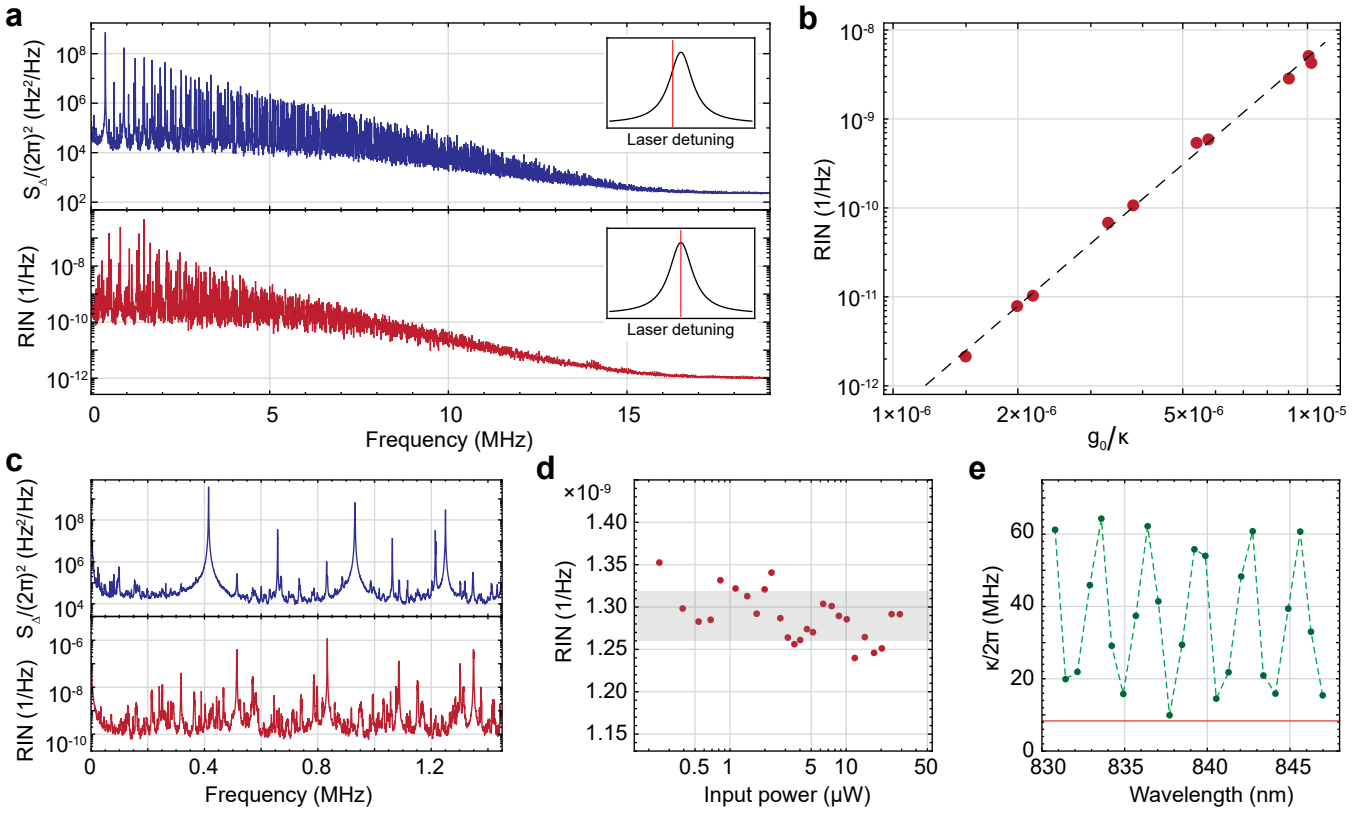

FIG. 2. a) Noise from a MIM cavity with laser detuned from resonance and on resonance. 1 mm square membrane, $\kappa/2\pi = 26.6$ MHz, $g_0/2\pi = 330$ Hz. c) The low frequency part of data in a). b), d) and e) show measurements for MIM cavity with 2 mm square membrane. b) dependence of the average RIN in $0.6-1.6$ MHz band. b) Power sweep on the resonance with wavelength 837.7 nm, band $\pm$ one standard deviation around the mean is shaded gray. e) Green points — measured linewidths of different optical resonances of MIM cavity, the dashed line is a guide to eye. Orange line — linewidth of an empty cavity with the same length.

The fluctuations of δ due to the mechanical displacement are given by

$$\delta(t) \approx \frac{G}{\kappa}x(t) + \frac{G_2}{2\kappa}x(t)^2, \tag{6}$$

where $G = -\partial\omega_c/\partial x$ and $G_2 = -\partial^2\omega_c/\partial^2 x$ are the linear and quadratic optomechanical coupling, respectively. So overall we have

$$a(t) \approx \frac{2}{\sqrt{\kappa}}\sqrt{\eta_1}(1 - i\delta(t) - \delta(t)^2)s_{1,\mathrm{in}} \approx \frac{2}{\sqrt{\kappa}}\sqrt{\eta_1}\left(1 - i\frac{G}{\kappa}x(t) - \left(\left(\frac{G}{\kappa}\right)^2 + i\frac{G_2}{2\kappa}\right)x(t)^2\right)s_{1,\mathrm{in}}. \tag{7}$$

It is instructive to compare the magnitudes of the two contributions to the prefactor of $x(t)^2$. The typical value for G (assuming the membrane to be approximately in the cavity center) is

$$G \sim 2r\frac{\omega_c}{L}, \tag{8}$$

while the typical value for G_2 is[20]

$$G_2 \sim 4\frac{r\omega_c^2}{Lc}, \tag{9}$$

so that the ratio of the two contributions can be evaluated as

$$\left(\frac{G}{\kappa}\right)^2 / \left(\frac{G_2}{2\kappa}\right) \sim \mathcal{F}r. \tag{10}$$

As the cavity finesse $\mathcal{F}$ is typically large, on on the order of 10^3 to 10^5, and the membrane reflectivity r is between 0.1 and 0.5, we conclude that linear optomechanical coupling needs to extremely well suppressed in order for the quadratic coupling G_2 to play any role. In the following we neglect G_2.

Next we calculate the spectrum or photocurrent fluctuations in the setting relevant to our experiment, when the laser is coupled to the cavity from port one and the output of the second port is detected by a photodiode. For the output field we have

$$s_{2,\mathrm{out}}(t) = -2\sqrt{\eta_1\eta_2}L(\delta(t))s_{1,\mathrm{in}}, \tag{11}$$

and for the photocurrent in direct detection

$$I(t) = |s_{2,\mathrm{out}}(t)|^2 \propto |L(\delta_0)|^2 \times \left(1 - \frac{2\delta_0}{1+\delta_0^2}\frac{G}{\kappa}x(t) + \frac{3\delta_0^2 - 1}{(1+\delta_0^2)^2}\left(\frac{G}{\kappa}\right)^2 x(t)^2\right), \quad (12)$$

where $\delta_0 = \Delta_0/\kappa$ is the average laser detuning from the resonance.

The frequency spectrum of the quadratic component of the photocurrent signal can be found using Wick's theorem

$$S_2[\omega] = \int_{-\infty}^{\infty} \langle x(t)^2 x(t+\tau)^2 \rangle e^{i\omega\tau} d\tau = 2\pi \langle x^2 \rangle^2 d[\omega] + 2 \times \frac{1}{2\pi}\int_{-\infty}^{\infty} S_1[\omega'] S_1[\omega - \omega'] d\omega', \quad (13)$$

where $d[\omega]$ is delta-function. If the cavity transduces the motion of multiple mechanical modes, the convolution results the appearance of frequency components at sum and difference frequencies, as illustrated in Fig. 1b. The quadratic spectrum of such system is dominated by intermodulation noise.

III. EXPERIMENTAL OBSERVATION OF EXTRANEOUS AMPLITUDE NOISE

A startling manifestation of the optical transduction nonlinearity is the emergence of thermal amplitude noise in the field, output from an optomechanical cavity under resonant optical excitation. In the conventional picture of linear optomechanics, intensity fluctuations of the light that goes out of the cavity under such conditions is shot noise limited or contains a small portion of thermal signal transduced by dissipative coupling. In reality, however, the intensity of light can contain of vast amount of thermal intermodulation noise. We study this noise systematically with rectangular membranes in the low-cooperativity regime.

Our experimental setup consists of a membrane in the middle cavity, composed of two supermirrors with the transmission of 100 ppm and a 200 um-thick silicon chip sandwiched between them that hosts a suspended high-stress silicon nitride membrane (see Fig. 1c). The membrane in the middle cavity is situated in a vacuum chamber at room temperature, it is probed using the light form a Ti:Sa or a tunable ECDL laser with wavelength around 840 nm. The Ti:Sa laser is used for noise measurements, whereas the diode laser is used only for the characterization of optical linewidths. The light reflected from the cavity is used for PDH locking, whereas the light exiting the cavity from the second port and detected in direct detection constitutes our measurement signal.

While reaching the quatum regime of optomechnaical interaction requires engineering high-Q and low mass mechanical oscillators, we perform the characterization of thermal intermodulation noise in low-cooperativity regime using conventional 20 nm-thick square membranes. In order to eliminate the influence of dynamic backaction, while characterizing the noises we keep the residual pressure in the vacuum chamber high, in the range 0.22 ± 0.03 mBar, so that the quality factor of the fundamental membrane mode is gas-damping limited to $Q \sim 10^3$.

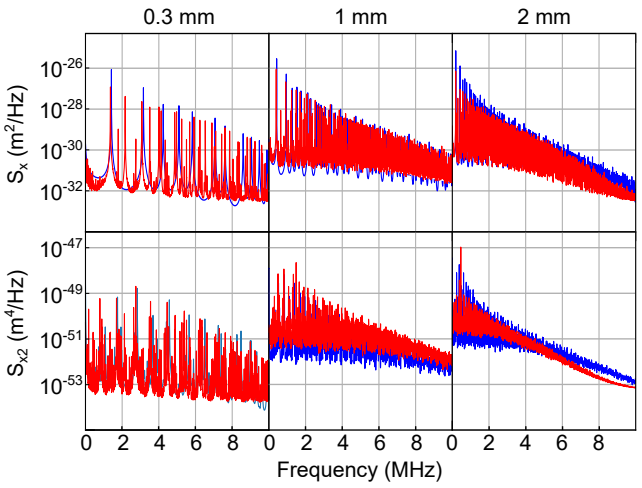

FIG. 3. Cavity-waist averaged position (top row) and position squared (bottom row) noises produced by the modes of 20-nm Si_3N_4 rectangular membranes of different sizes. Red is experimental data and blue is theoretical prediction. (Warning: two-sided theory spectra might be plotted, also the data for 2 mm membrane should be replaced)

We start by presenting in Fig. 2a and c the observation of strong classical amplitude noise in the output from the cavity subjected to resonant optical excitation. For MIM cavity with 1mm × 1mm × 20nm membrane and the input power of 5 μW the classical amplitude noise rises above the shot noise level by about 25 dB at low frequencies. In Fig. 2a, the noise level approaches shot noise at high frequencies due to averaging of the membrane mode profiles of the cavity waist (approx 25 μm in our experiment).

Next we prove that the observed amplitude noise originates from the nonlinearity of cavity transduction by performing noise measurements across different optical resonances of the same cavity and referring the amplitude noise level to the value of vacuum optomechanical coupling rate of the fundamental mode over the optical linewidth (see Fig. 2b). We use a 2mm × 2mm × 20nm membrane for this measurement. While the power spectral density of linearly transduced thermal fluctuations is $\propto (g_0/\kappa)^2$, the spectral density of quadratically transduced noise is $\propto (g_0/\kappa)^4$, a trend that is perfectly consistent with the data in Fig. 2b. By performing a sweep of the input laser power on one of the resonances (see Fig. 2d) we show that the intermodulation noise level is power-independent and therefore the observed noise is not related to the optomechanical dynamic backaction, negligible for the operation in low vacuum.

The intermodulation noise observed in our experiment is well reproduced by a theoretical model with no fitting parameters. The frequency noise produced by the thermal membrane motion in a MIM cavity can be found as

$$S_\Delta[\omega] = G^2 \sum_n A_n^2 S_{x,n}[\omega], \tag{14}$$

where $S_{x,n}[\omega]$ are the displacement noises of individual membrane modes and A_n are the factors characterizing the signal low-pass filtering due to the geometric overlap of mechanical mode profiles with the optical mode and due to the finite cavity response time. In our experiment the effect of finite cavity response time is small compared to the effect of geometric overlap, but we still take it into account. By using Eq. 12 and Eq. 13 we can find the spectrum of quadratically tansduced fluctuations and the resulting amplitude noise given the spectrum of cavity frequency fluctuations from Eq. 14. We present a comparison between experimentally measured linear and quadratic displacement noise spectra and the ones calculated using the theoretical model in Fig. 3. The inputs for the model in this case are experimentally measured g_0 of the fundamental membrane mode, the optical linewidth κ, the membrane size and its quality factors (for simplicity, assumed to be the same for all the modes). While our model is not detailed enough to reproduce precisely all the noise features, it well reproduces the overall level and the broadband envelope of the intermodulation noise that were observed in experiment.

IV. INTERMODULATION NOISE IN AN OPTOMECHANICAL CAVITY WITH A PHONONIC CRYSTAL MEMBRANE

The quantum regime of optomechanic interaction, when the radiation pressure shot noise matches the thermal force noise, is reached at the input laser power given by

$$P_{\text{in}} = \frac{\pi c}{32\hbar} \frac{\lambda}{\mathcal{F}^2} \frac{S_{\text{FF,th}}}{4r^2}, \tag{15}$$

where it is assumed that the membrane is positioned along the cavity to maximize the linear optomechanical coupling, λ is the optical wavelength, $\mathcal{F}$ is cavity finesse, r is membrane reflectivity and $S_{\text{FF,th}}$ is the thermal force noise spectral density given by[24]

$$S_{\text{FF,th}} = 2k_B T m_{\text{eff}} \Gamma_m. \tag{16}$$

The reduction of thermal noise is essential for reaching the quantum backaction-dominated regime. Recently thermal noise down to 55 aN/$\sqrt{\text{Hz}}$ was demonstrated at room temperature for soft-clamped modes localized in stressed phononic crystal membrane nanoresonators[25, 26], owing to the simultaneous enhancement of quality factor and the reduction of effective mass. Although similar force noise levels are attainable with trampoline resonators[22], the advantage of soft-clamped localized modes is their high frequency, on the order of MHz, which makes them less affected by classical laser noises. Even lower thermal noise, down to 10 aN/$\sqrt{\text{Hz}}$, was demonstrated for soft-clamped modes in nanobeam[27] resonators, but nanobeams are not straightforward to combine with Fabry-Perot cavities.

The integration of a membrane resonator with a Fabry-Perot optical cavity generally involves tradeoffs for the attainable thermal noise. Practical constraints need have to be satisfied include maintaining a good overlap between the mechanical mode and the optical cavity waist and ensuring that the mechanical mode of interest is spectrally well isolated from other membrane modes.

In Fig. 4a and b we present designs of PnC membranes with defects optimized to create low effective mass and high-Q soft-clamped modes. The phononic crystal is made by a hexagon pattern of circular holes, which was introduced in Ref. [25] and makes the simplest arrangement that creates a complete phononic bandgap for the flexural modes. The phononic crystal is terminated to the frame at half the hole radii, which is necessary to avoid the appearance of modes, localized at the membrane edges—such modes have frequencies withing the phononic bandgap and can contaminate the mechanical spectrum.

Fig. 4a shows the microscope image of a resonator with trampoline defect, featuring a particularly low $m_{\text{eff}} = 1.9$ ng at $\Omega_m/2\pi = 0.853$ kHz and $Q = 1.65\times10^8$, corresponding to the force noise of $S_{\text{FF,th}} = 15$ aN/$\sqrt{\text{Hz}}$. Another design, shown in Fig. 4d, is a 2 mm by 2 mm by 40 nm phononic crystal membrane with defect in the center that was engineered to create a single mode localized in the middle of phononic bandgap. This design features $Q = 4.1 \times 10^7$ at 1.5 MHz and the effective mass of 2.2 ng, which results in predicted $S_{\text{FF,th}} = 200$ aN/$\sqrt{\text{Hz}}$. The overall membrane size in this case of the second design is kept small enough so that no other modes, including in-plane ones, fall into the phononic bandgap. The complete membrane designs is available from Zenodo repository[28].

Using the membrane shown in Fig. 4d we were able to reproducibly assemble membrane-in-the-middle cavities with single-photon cooperativity $C_0 = 0.1 - 1$ (when operated in high vacuum, around 4×10^{-7} mBar in our case) and round trip loss lower than 200 ppm. According to the estimate provided by Eq. 15, in such cavities the quantum backaction-dominated regime is expected to be reached at the input powers of a few hundreds of μW. Our experiment, however, shows that at these powers the optical amplitude noise in such cavities is far from being limited by the vacuum fluctuations of light due to the intermodulation noise. The latter is big challenge for the exploration of quantum aspects of radiation pressure interaction at room temperature.

Fig. 4e shows the spectrum of light output from a membrane in the middle cavity with length around 350 μm, $g_0/2\pi = 360$ Hz, $\kappa/2\pi = 24.8$ MHz and the intrinsic loss

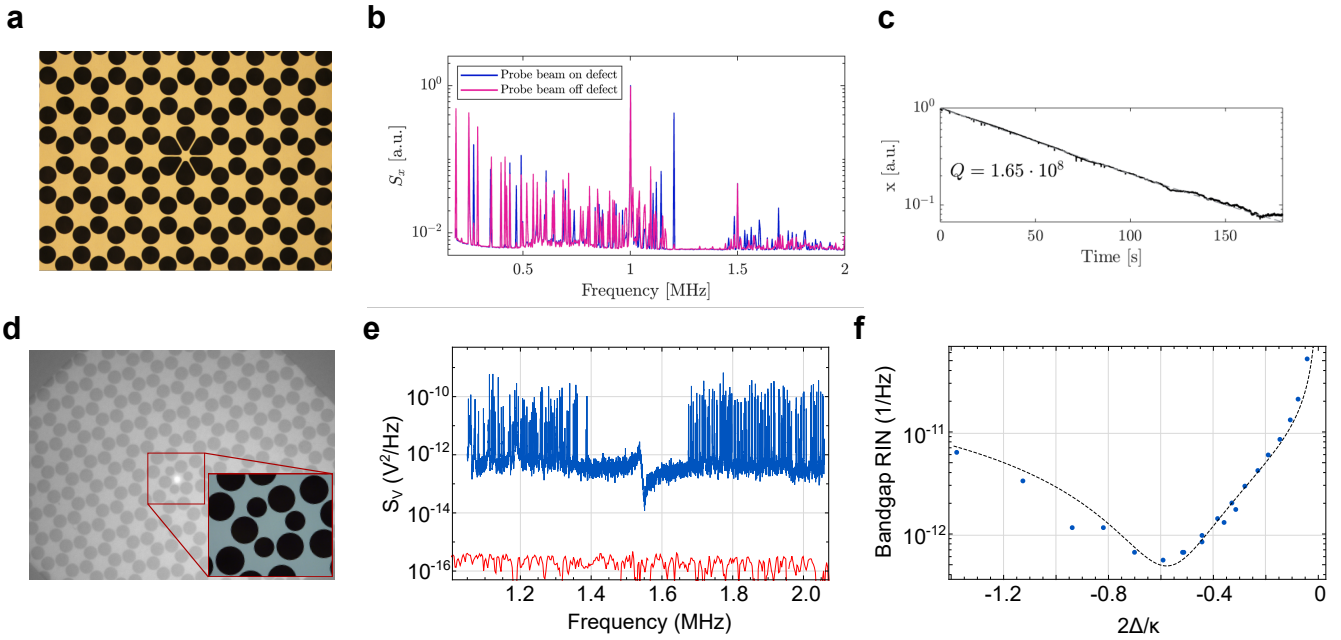

FIG. 4. a) Microscope image of a 3.6mm ×3.3mm × 20nm, with a low m_{eff} localized mode frequency of approximately 800 kHz, b) displacement spectrum of the membrane in a(replace data for this to be true) c) ringdown measurement of quality factor of the membrane in a. d) Microscope image of a 2mm × 2mm × 20nm membrane hosting a soft clamped mode. e) Blue—protocurrent noise spectrum detected with laser detuned from the cavity resonance, red—shot noise level. f) The variation of the relative intensity noise of the light output from MIM cavity at bandgap frequencies with laser-cavity detuning. Blue dots are experimental points, dashed line - single-parameter model fit.

rate around 100 ppm, close to the output coupling rate from the two cavity mirrors having the transmission of 100 ppm each. The laser was detuned to the red from the cavity resonance in this measurement, and the spectrum of output fluctuations contains both the contribution of thermomechanical noise linearly transduced by the cavity detuning and the intermodulation noise due to the nonlinearity in G/κ. In particular, at frequencies within the phononic bandgap the noise level is dominated by the intermodulation noise, which rises almost 40 dB above the level of vacuum fluctuations (calibrated separately by directing an auxiliary laser beam of the the same power on the detector). The intermodulation origin of the noise in the bandgap can be proven by considering the variation of the noise level with laser detuning presented in Fig. 4f. The laser power in this measurement was kept fixed to 30 μW, the cavity resonance wavelength is 840.1 nm.

We can understand the data in Fig. 4f using the general formula for the photocurrent produced in the detection of outgoing light (Eq. 12). Linear and quadratic position fluctuations are transduced differently by the cavity, but almost within the entire range of the detunings the quadratically transduced fluctuations dominate. The exception is the vicinity of the detuning $\Delta = \kappa/(2\sqrt{3})$ at which the quadratic transduction by the cavity is compensated by the quadratic transduction by the nonlinearity of photodetection (see SI for discussion). At this detuning the in-bandgap noise level is consistent with the mirror noise. The overall variation of noise with the detuning can be described by the formula

$$S_{\text{RIN}} \propto \frac{4\delta_0^2}{(1+\delta_0^2)^2} S_1 + \frac{1}{\delta_0}\frac{(3\delta_0^2-1)^2}{1+\delta_0^2} S_2, \qquad (17)$$

where S_1 is the contribution of mirror noise, which is independently calibrated, and S_2 is the contribution of quadratic noise that we use as a fitting parameter for the dashed curve in Fig. 4f. Aside from the cavity transduction, Eq. 17 takes into account the laser cooling of mechanical modes by dynamic backaction (assuming that the optical damping is much larger than the intrinsic linewidth, see SI for details). As can be seen from Fig. 4f, Eq. 17 very well reproduces the experimental data.

V. ACKNOWLEDGEMENTS

This work was supported by...

[1] H. Miao, S. Danilishin, T. Corbitt, and Y. Chen, Physical Review Letters **103**, 100402 (2009).

[2] F. Khalili, S. Danilishin, H. Miao, H. Mller-Ebhardt, H. Yang, and Y. Chen, Physical Review Letters **105**,

070403 (2010).
[3] A. A. Gangat, T. M. Stace, and G. J. Milburn, New Journal of Physics **13**, 043024 (2011).
[4] A. A. Clerk, F. Marquardt, and J. G. E. Harris, Physical Review Letters **104**, 213603 (2010).
[5] A. Nunnenkamp, K. Brkje, J. G. E. Harris, and S. M. Girvin, Physical Review A **82**, 021806 (2010).
[6] I. Martin and W. H. Zurek, Physical Review Letters **98**, 120401 (2007).
[7] G. A. Brawley, M. R. Vanner, P. E. Larsen, S. Schmid, A. Boisen, and W. P. Bowen, Nature Communications **7**, 10988 (2016).
[8] T. K. Paraso, M. Kalaee, L. Zang, H. Pfeifer, F. Marquardt, and O. Painter, Physical Review X **5**, 041024 (2015).
[9] R. Leijssen, G. R. L. Gala, L. Freisem, J. T. Muhonen, and E. Verhagen, Nature Communications **8**, 1 (2017).
[10] A. H. Safavi-Naeini, S. Grblacher, J. T. Hill, J. Chan, M. Aspelmeyer, and O. Painter, Nature **500**, 185 (2013).
[11] T. P. Purdy, P.-L. Yu, R. W. Peterson, N. S. Kampel, and C. A. Regal, Physical Review X **3** (2013), 10.1103/PhysRevX.3.031012.
[12] J. Chan, T. P. M. Alegre, A. H. Safavi-Naeini, J. T. Hill, A. Krause, S. Grblacher, M. Aspelmeyer, and O. Painter, Nature **478**, 89 (2011).
[13] D. J. Wilson, V. Sudhir, N. Piro, R. Schilling, A. Ghadimi, and T. J. Kippenberg, Nature **524**, 325 (2015).
[14] M. Rossi, D. Mason, J. Chen, Y. Tsaturyan, and A. Schliesser, Nature **563**, 53 (2018).
[15] T. P. Purdy, K. E. Grutter, K. Srinivasan, and J. M. Taylor, arXiv:1605.05664 [cond-mat, physics:physics, physics:quant-ph] (2016), arXiv: 1605.05664.
[16] V. Sudhir, R. Schilling, S. Fedorov, H. Schtz, D. Wilson, and T. Kippenberg, Physical Review X **7**, 031055 (2017).
[17] J. Cripe, N. Aggarwal, R. Lanza, A. Libson, R. Singh, P. Heu, D. Follman, G. D. Cole, N. Mavalvala, and T. Corbitt, Nature **568**, 364 (2019).
[18] M. J. Yap, J. Cripe, G. L. Mansell, T. G. McRae, R. L. Ward, B. J. J. Slagmolen, P. Heu, D. Follman, G. D. Cole, T. Corbitt, and D. E. McClelland, Nature Photonics , 1 (2019).
[19] N. Aggarwal, T. Cullen, J. Cripe, G. D. Cole, R. Lanza, A. Libson, D. Follman, P. Heu, T. Corbitt, and N. Mavalvala, arXiv:1812.09942 [physics, physics:quant-ph] (2018), arXiv: 1812.09942.
[20] J. D. Thompson, B. M. Zwickl, A. M. Jayich, F. Marquardt, S. M. Girvin, and J. G. E. Harris, Nature **452**, 72 (2008).
[21] D. J. Wilson, C. A. Regal, S. B. Papp, and H. J. Kimble, Physical Review Letters **103**, 207204 (2009).
[22] C. Reinhardt, T. Mller, A. Bourassa, and J. C. Sankey, Physical Review X **6**, 021001 (2016).
[23] A. B. Matsko and S. P. Vyatchanin, Physical Review A **97**, 053824 (2018).
[24] P. R. Saulson, Physical Review D **42**, 2437 (1990).
[25] Y. Tsaturyan, A. Barg, E. S. Polzik, and A. Schliesser, Nature Nanotechnology **12**, 776 (2017).
[26] C. Reetz, R. Fischer, G. Assumpo, D. McNally, P. Burns, J. Sankey, and C. Regal, Physical Review Applied **12**, 044027 (2019).
[27] A. H. Ghadimi, S. A. Fedorov, N. J. Engelsen, M. J. Bereyhi, R. Schilling, D. J. Wilson, and T. J. Kippenberg, Science **360**, 764 (2018).
[28] Raw measurements data, analysis code to repoduce the manuscript figures, and the GDS designs of PnC membranes are available on zenodo.org, DOI:.../zenodo....